International Journal of Earth Sciences Knowledge and Applications
journal homepage: http://www.ijeska.com/index.php/ijeska

Research Article

e-ISSN: 2687-5993

Evaluating the Effects of Land Use and Land Cover Change on Watershed Surface Runoff: Case of Abelti Watershed, Omo Basin, Ethiopia

Melkamu Ateka[1], Ligalem Agegn[1], Alemshet Belayneh[2]*

[1]*Faculty of Water Resources and Irrigation Engineering, Arbaminch Water Technology Institute, Arbaminch University, Arbaminch, Ethiopia*
[2]*Department of Water Resources and Irrigation Engineering, Institute of Technology, Woldia University, P.O. Box 400, Woldia, Ethiopia*

INFORMATION

Article history
Received 27 April 2021
Revised 03 May 2021
Accepted 20 May 2021

Keywords
Abelti watershed
Earth Resources Development Assessment System
Land Use/Land Cover
Surface runoff
SWAT model

Contact
*Alemshet Belayneh
alembe29@gmail.com

ABSTRACT

This study assessed the effects of land use/land cover change on surface runoff in Abelti watershed located at upper Omo river basin, Ethiopia using Soil and Water Assessment Tool and satellite land use maps of 2000, 2010 and 2017 which were processed using Earth Resources Development Assessment System, Imagine 2015 and ArcGIS10.1 software by the method of supervised classification. There was significant change surface runoff in the watershed due to spatial and temporal change of land use/land cover change. Surface runoff was very high during wet seasons and very low during dry seasons at different parts of the watershed during the study periods. Accuracy assessment of land use classification using confusion matrix and kappa coefficient for 2000, 2010 and 2017 maps indicated an overall accuracy of 86.04%, 90.75% and 89.71% and kappa index of 0.82, 0.88 and 0.86 respectively and image classification accuracy was almost in strong agreement. The model performance was found very well according to the three objective functions of R^2, Nash, Sutcliffe Efficiency and Percent Bias with values of 0.79, 0.78 and 6.3% for calibration and 0.92, 0.85 and 4.1% for validation periods respectively. Land cover types contribute minimum and maximum surface runoff based on the interception capacity of each land cover types in the watershed. Along with land use/land cover changes, considerable consequences were obtained in the surface runoff of the watershed which was increased from 2000 to 2010 by 19.963% but decreased from 2010 to 2017 by 3.898% due to change of land use/land cover in the watershed. Therefore, surface runoff was highly affected by land cover types and increased when the interception was less because of the forest cover decreased, surface runoff decreased when the forest cover become increased.

1. Introduction

Hydrological models are powerful technique of hydrologic system investigation and simplified representation of real-world system which give results close to reality with the use of input parameters (Gayathri et al., 2015). Hydrologic modelling and studies of water resources management were inter-related with each other to the spatial process of the hydrologic cycle at basin, watershed and sub-watershed level (Samuel et al., 2018). A major land part of the country is being used by small holder farmers who farms the land for food to stay alive. With the dynamic growth of the population and without agricultural intensification, smallholders need more land to irrigate crops and get a living (Hadgu, 2008).

The land use/land cover (LULC) change often leads to undesirable consequences that negatively impact functioning of natural ecosystems and human beings themselves. The impacts could be manifested across a wide spectrum of environmental systems including the atmospheric, hydrologic and ecological systems (Chalachew et al., 2015).

Understanding the impacts of land use changes on surface runoff is important to know the impacts of LULC changes on watershed surface runoff. Along with LULC changes, considerable outcomes were expected for hydrological process and subsequent impacts on water resources (Githu, 2007). LULC change is therefore, a critical environmental and socio-economic issue that requires research attention.

Natural land cover can be changed due to dynamic population growth, deforestation, agricultural expansion, improper land management (Alemu, 2015).

The assessment and identifying land cover change needs correct or accurate evaluation of the type and direction of changes happening in the Abelti Watershed of Omo Basin through change assessment of images of remotely sensed LULC maps of 2000, 2010 and 2017. Different methods of quantification were used to handle spatial data capabilities of Geographic Information Systems (GIS) to process data. These were done by integrating Earth Resources Development Assessment System (ERDAS) imagine 2015 with GIS 10.1 to run, quantify and identify land cover changes. Finally, to reveal information for the status of LULC map classification to be used as in put for Soil and Water Assessment Tool (SWAT) model simulation and calibration to analysis and compare land use change impact on surface runoff accuracy assessment was done.

Several studies were carried in the watershed to identify factors affecting soil erosion, sedimentation problems and LULC class analysis on Omo Basin for a long period of times whereas this study will focus on the upper part of the basin in the sub-watershed level and identify effects of LULC changes of surface runoff for the watershed using SWAT model and ERDAS imagine 2015. Not only this but also the study located the place where maximum surface runoff was found in the Abelti Watershed but none of the above scholars discussed about the sever areas of the study area.

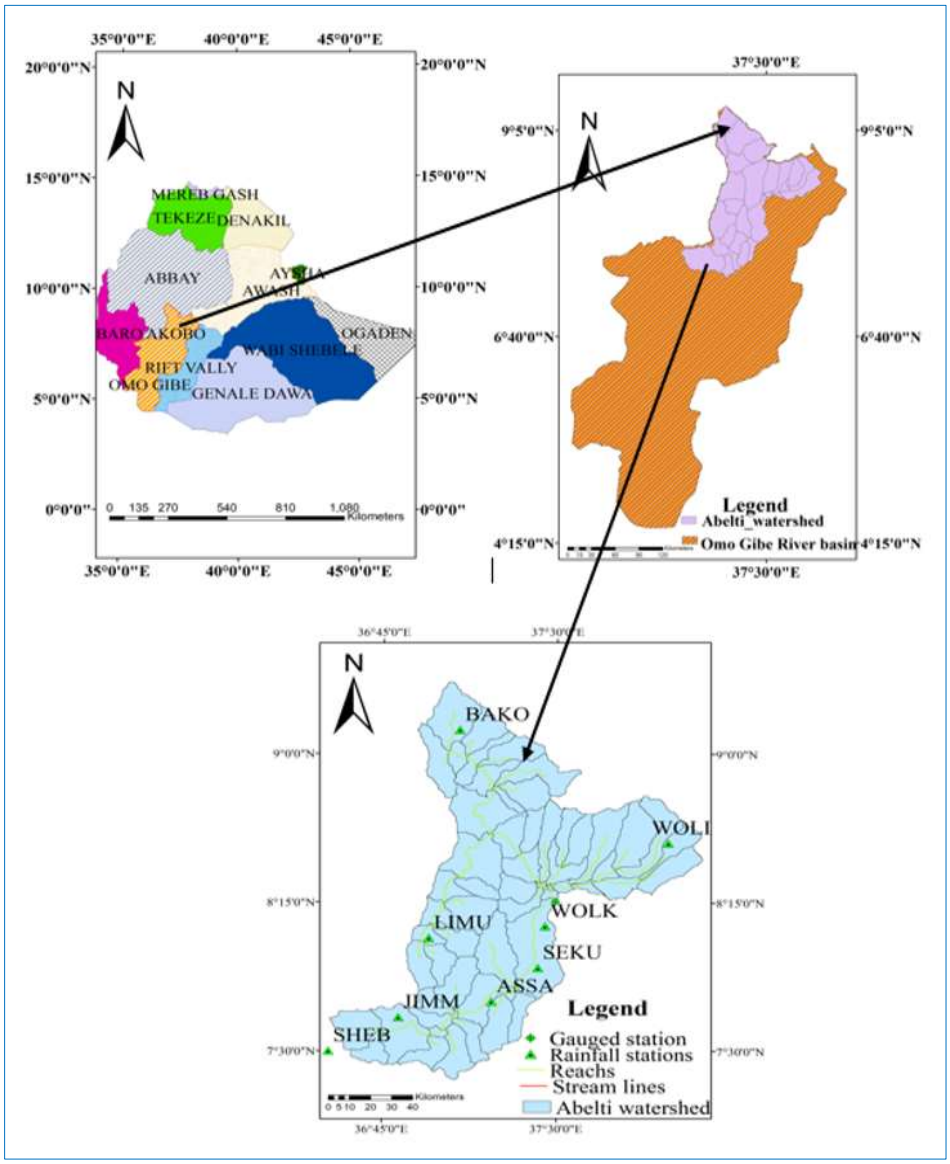

Fig. 1. Location and description map of the study area

2. Materials and Methods

2.1. Study area description

The location of Abelti watershed is in the upper Omo Gibe Basin in the 7.35ºN-9.36ºN latitude and 36.5ºE-38.13ºE longitude in Ethiopia. It is the main tributary for the Omo Gibe Basin with maximum and minimum elevation of 3259m and 1090m respectively. Gilgel Gibe River is found in the watershed with an important Contributor compare to the

other with a drainage area of 15374 km^2. The flow direction of Gibe River is southwards, to the Omo River and to Lake Turkana a faulty feature (RichardWoodroof and Associates, 1996). In Fig. 1, the location and description map of the study area is presented.

2.2. Climate and hydrological data

Omo-Gibe River Basin differs from temperate/hot arid climate properties from southern part of the floodplain to tropical humid of the highlands which include extreme north as well as northwestern part of Omo Basin. Intermediate between these variable climate properties and for the largest part of the basin climate is tropical sub-humid (RichardWoodroof and Associates, 1996). In Figs. 2, 3 and 4, the distribution of rainfall (monthly and yearly) and temperature is described.

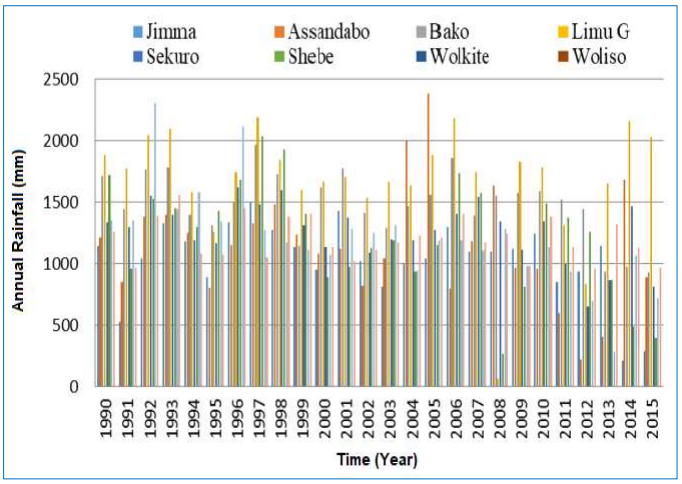

Fig. 2. Annual rainfall distribution of meteorological stations

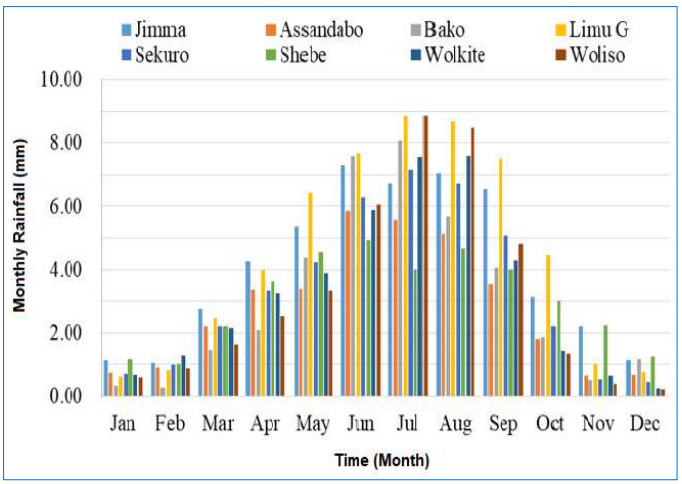

Fig. 3. Average monthly rainfall stations of the watershed

Flow data were collected for hydrological model validation and calibration from 1999-2015 years daily based of the watershed from Ethiopian ministry of water irrigation and energy and arranged as required by SWAT model used for sensitivity analysis, calibration and validation. In Fig. 5, hydrological data is presented.

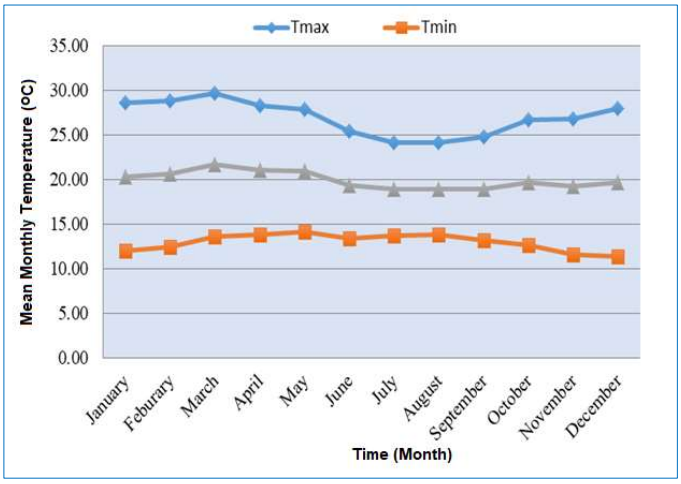

Fig. 4. Long-term mean monthly max. and min. temperature of stations

2.3. Data type and sources

This study focusses on the use of distributed physically based hydrological model which requires hydro-meteorological and spatial input data as shown in the Table 1.

2.3.1. Digital Elevation Model (DEM)

Digital elevation model is used as input for SWAT model to develop sub-watershed or delineate watershed into different sub-watersheds and drainage patterns of the watershed, stream lengths and widths of channel within the watershed were developed from DEM.

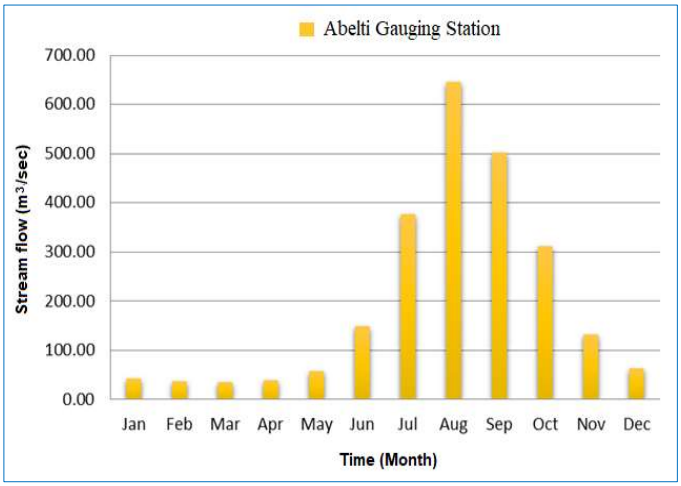

Fig. 5. Mean monthly stream flow of Abelti Gauging Station

2.3.2. Soil data

Soil map of study area was collected from Ethiopian Ministry of Water, Irrigation and Energy (MoWIE) and fourteen major soil groups were identified using the shape file of Abelti Watershed available water content, bulk density, soil texture, hydraulic conductivity and different organic carbon content for layers of each soil type was extract (FAO,1995) as shown Table 2.

2.3.3. LULC

LULC map is very important input for hydrological model

SWAT to determine the impacts on watershed hydrology and explain hydrological response units of the watershed. Classification of land use map was prepared to represent the LULC according to the information from USGS Earth Explore. Six various types or classes of LULC were differentiated for the study area as shown in Fig. 6.

Table 1. List of data type and data sources

Category	Data type	Data sources	Used
Temporal data	Meteorological data ✓ Rainfall ✓ Max. and min. temperature ✓ Relative humidity ✓ Sun shine hour ✓ Wind speed	MoWIE	Model simulation
Spatial data	Hydrological data ✓ Stream flow	MoWIE	Model calibration and validation
	✓ DEM (30x30) ✓ Soil	MoWIE	To know drainage pattern and stream lengths and model simulation
	✓ LULC of 200, 2010 and 2017 (From Satellite)	USGS Earth Explorer	Model simulation

Table 2. Soil of the watershed with their aerial coverage (MoWIE)

Soil type	Area, km^2	Area, %
Calaricflubisols	114	0.74
Chromicvertisols	1.261	8.20
Chromiccambisols	3	0.02
Chromicluvisols	549	3.57
Eutricnitisols	1.307	8.50
Eutricfluvisols	527	3.43
Gypsicyermosols	3	0.02
Dystricnitisols	4.822	31.36
Eutriccambisols	9	0.06
Pellicvertisols	3.423	22.26
Leptosols	18	0.12
Dystricfluvisols	1.377	8.96
Orthicluvisols	1.011	6.58
Orthicacrisols	950	6.18

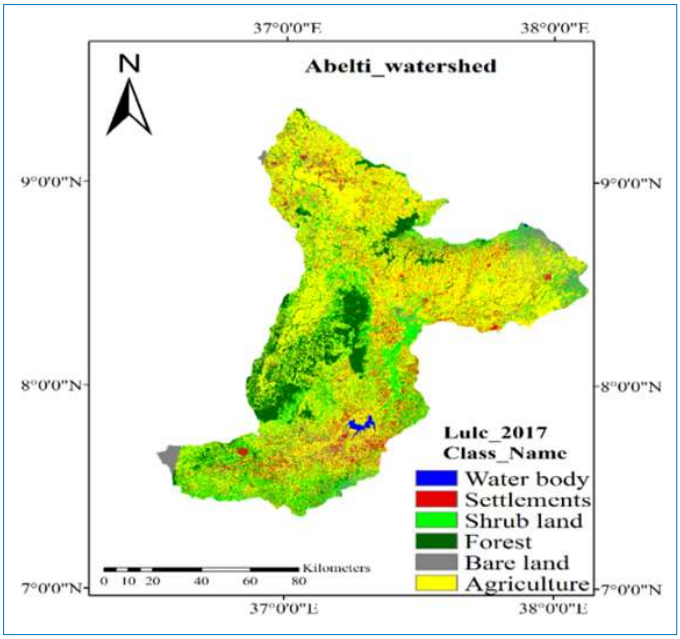

Fig. 6. Prepared or classified LULC map of the watershed for 2017

2.4. Data Quality Test

2.4.1. Checking homogeneity

Checking homogeneity of selected stations of monthly rainfall records was done by non-dimensionalzing by using the following relation and consistent record is one at which the properties of the record have not varied with time as shown Fig. 7.

$$Pi = \frac{Piavg}{Pavg} * 100 \quad (1)$$

where; P_i is value of non-dimensional precipitation for the month i, P_{iavg} is monthly average precipitation of station i and P_{avg} is yearly average precipitation of the stations.

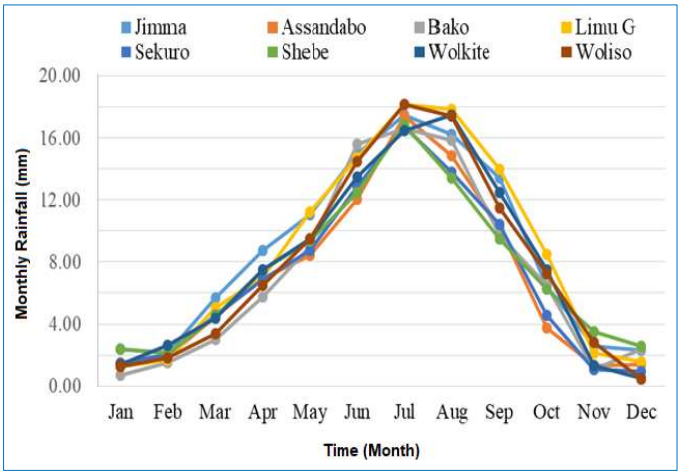

Fig. 7. Homogeneity Test for rainfall stations

2.4.2. Consistency

Spatial consistency of the precipitation data and all the selected stations in this study were consistent using correlation coefficient and checked by using double mass curve (DMC) as shown in the Fig. 8.

2.5. Classification of LULC

Processes/classification were performed by using remotely sensed Landsat satellite imageries using ERDAS2015 image

processing and ArcGIS10.1 spatial analysis interfaces were used to reclassify remotely sensed imagery data to detect change of the LULC of study area. Satellite image data were downloaded in the form of zipped files by using United States geological survey/USGS link/web to tiff format files as shown Table 3.

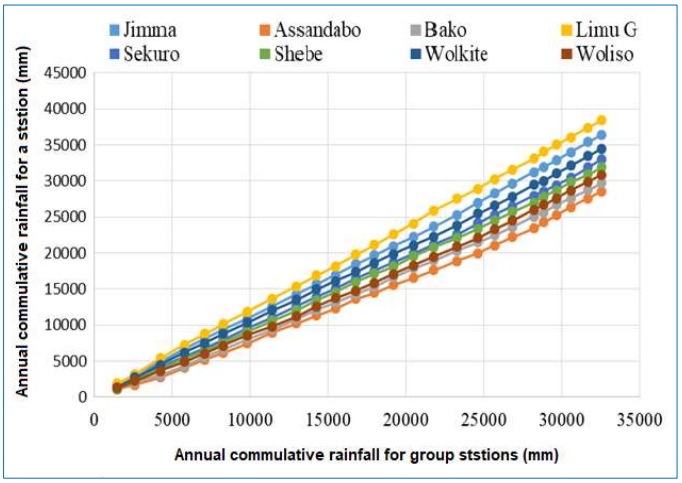

Fig. 8. Test for consistence of rainfall station by using DMC method

Table 3. Sensor, acquisition date, resolution, producer and path/row of the image

Path/Row	Acquisition date	Sensor	Resolution (m)	Producer
169/055	2000/01/27	ETM^{+}	30	USGS
169/055	2010/01/17	TM	30	USGS
169/055	2017/01/01	OLI	30	USGS

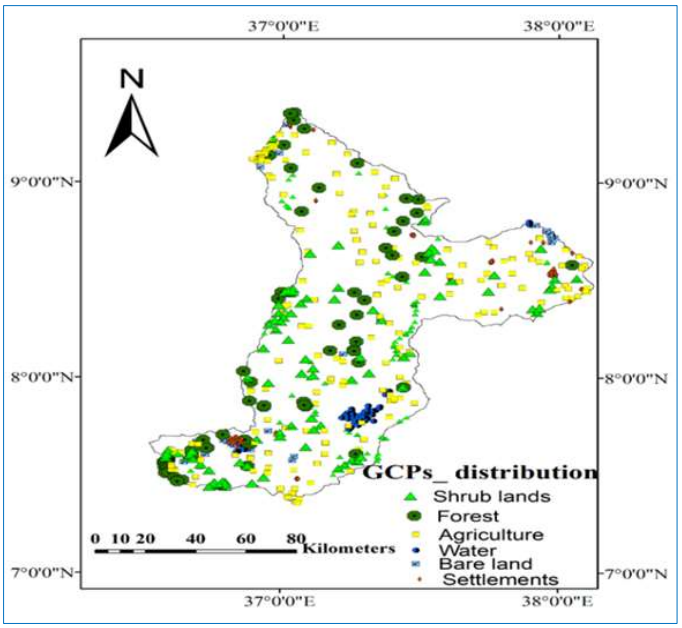

Fig. 9. Spatial distribution of GCPs in the watershed

2.5.1. Ground Control Points (GCPs)

GCPs were collected based on normalized difference vegetation index (NDVI) values of each land cover classes based on pixel value ranges of each class at which ground control points were taken to produce signature for supervised classification and accuracy assessment of classified LULC maps of the watershed. GCPs of the study area were distributed as shown in Fig. 9.

2.6. Assessment of accuracy for classified images

Classified images accuracy assessment is crucial for the process of satellite image classification. The main objective of accuracy assessment is to determine how effectively pixels were classified in to the right feature types for the area under investigated. Outcomes of images classification was validated using confusion matrix of which various accuracy tequnics can be developed (Rientjes et al., 2010). A confusion matrix lists the values for the classified data in the rows and for known land cover types of the reference data in the columns.

2.6.1. Kappa coefficient

Kappa coefficient is evaluation of a matrix overall agreement and it is ratio of the total of values of diagonal to total number of cell count for matrix (Susana et al., 2010).

$$Ka = \frac{N\sum_{i=1}^{r} Xii - \sum_{1=1}^{r} Xi + i + X}{N^2 - \sum_{i=1}^{r} Xi + i + X} \quad (2)$$

where; r is column and row number for error matrix, N is overall number of observed, Xii is observation in column i and row i, Xi is marginal total row i and i+X is marginal total column i.

2.7. SWAT theoretical frame work

SWAT is computationally efficient, physically based and able for continuous simulation for a long period of time (Palmer, 2002). SWAT Hydrologic simulation depends on water balance equation as shown below.

$$Swt = \sum_{i=1}^{t} (Rday - ET - Qsurf - Wseep - Qgw) + Swo \quad (3)$$

where; Swt is content of final soil water (mm), Swo is content of initial soil water for day i (mm), t is time (day), $Rday$ is magnitude of rainfall for day i (mm), $Qsurf$ is magnitude of surface runoff for day i (mm), ET is amount of evapotranspiration for day i (mm), $Wseep$ is magnitude of water entering into vadose zone from soil profile for day i (mm) and Qgw is magnitude of return flow for day i (mm).

2.7.1. Occurrence (generation) of surface runoff

Surface runoff or overland flow is a flow that happens through sloping surface and occur when the rate of water joined to the ground surface greater than the rate of infiltration and Surface runoff can also be generated by the method of Saturation excess overland flow or by infiltration excess overland flow method.

Surface runoff is the major element in the hydrologic process. The initial abstraction (Ia) is approximately equal to 0.2S and the method is an empirical model, which is based on the following equations:

$$Qsurf = \frac{(Rday - Ia)^2}{(Rday - Ia + S)} \quad (4)$$

but

$$S = 25.4\left(\frac{100}{CN} - 10\right) \quad (5)$$

and then

$$Qsurf = \frac{(Rday - 0.2S)}{(Rday + 0.8S)} \quad (6)$$

where; *Qsurf* is commutated rainfall excess or surface runoff (mm), *Rday* is depth of rainfall for the day (mm), *Ia* is initial abstraction with surface storage, interception and infiltration before to runoff (mm) and *S* is a holding parameter (mm).

2.8. General methodology

Flow chart of the adopted methodology and framework of the study was shown in Fig. 10.

2.9. Validation and calibration of model

2.9.1. Model validation

Model Validation was done to compare the result of model with independent data set without making additional adjustment of model parameter values.

2.9.2. Model calibration

Model calibration involves adjustment of model input parameters and comparison of results with observed values up to selected objective functions are achieved (James and Burges, 1982).

Following model sensitivity analysis, calibration of model was done to get optimum values for each sensitive parameter. The auto calibration tool in SWAT was run using SUFI-2 with uncertainty analysis mode using monthly average collected stream flow data of the study area.

2.9.3. Evaluation of model performance

Coefficient of determination (R^2) and Nash, Sutcliffe Efficiency (ENS) was used to determine model performance during the calibration and validation periods. Strength of relationship between the observed and simulated values were evaluated using the value of coefficient of determination (R^2= *0*, poor; R^2= *1*, good).

$$R^2 = \frac{\sum_{i=}^{n}[Xi - Xav] * [Yi - Yav]}{[\sqrt{\sum[Xi - Xav]^2} * \sqrt{\sum[Yi - Yav]^2}} \quad (7)$$

where; *Xi* is measured values (m^3/se), *Xav* is average measured values (m^3/sec), *Yi* is simulated values (m^3/sec) and *Yav* is average simulated values (m^3/sec).

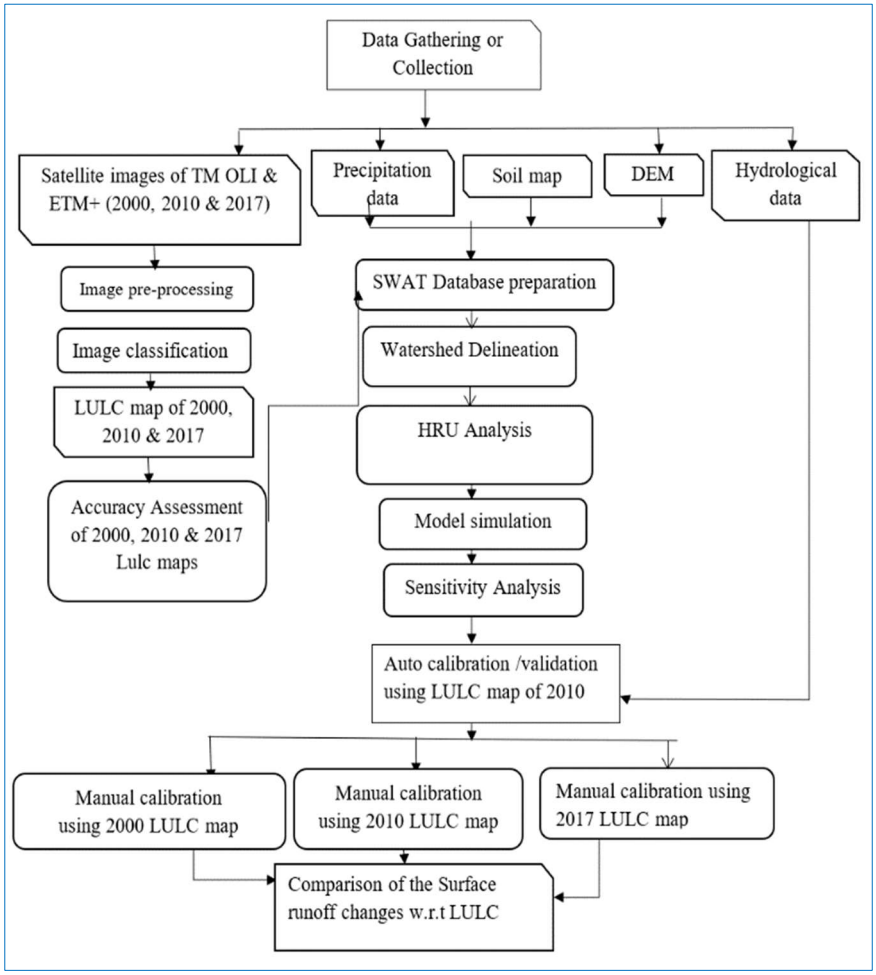

Fig. 10. Flow chart of the adopted methodology and framework of the study

2.9.4. ENS

Value of EBS shows that how well the plot of simulated versus observed value fits each other. If NSE is negative, predictions are poor and the average value of output is better predicts /estimate than the model prediction (Santhi et al., 2001).

$$ENS = 1 - \frac{\sum_{i=1}^{n}((Xi - Yi)^2)}{\sum_{i=1}^{n}((Xi - Xav)^2)} \quad (8)$$

where; *Xi* is measured values, *Yi* is simulated values and *Xav* is average observed values.

2.9.5. Percent Bias PBIAS

The PBIAS evaluates the average tendency of the simulated data to be more or less than the observed values and expressed in percentage the smaller the absolute value of the PBIAS is the better will be the model performance (Gupta et al., 1999).

$$PIAS = 100 * \left[\frac{(\sum_{i=1}^{n} qsim - \sum_{i=1}^{n} qoi)}{\sum_{i=1}^{n} qoi}\right] \quad (9)$$

where; q*sim* is the simulated discharge and *qoi* is the measured discharge.

According to Moriasi and Sanithi the model performance criteria is presented in Table 4.

Table 4. Evaluation criteria of model performance (Moriasi, 2007; Santhi et al., 2001)

Rating	R^2	ENS	PBIAS
Very good	0.75-1	0.75-1	<10%
Good	0.65-0.75	0.65-0.75	10%-15%
Satisfactory	0.5-0.65	0.5-0.65	15%-25%
Unsatisfactory	<0.60	<0.50	>25%

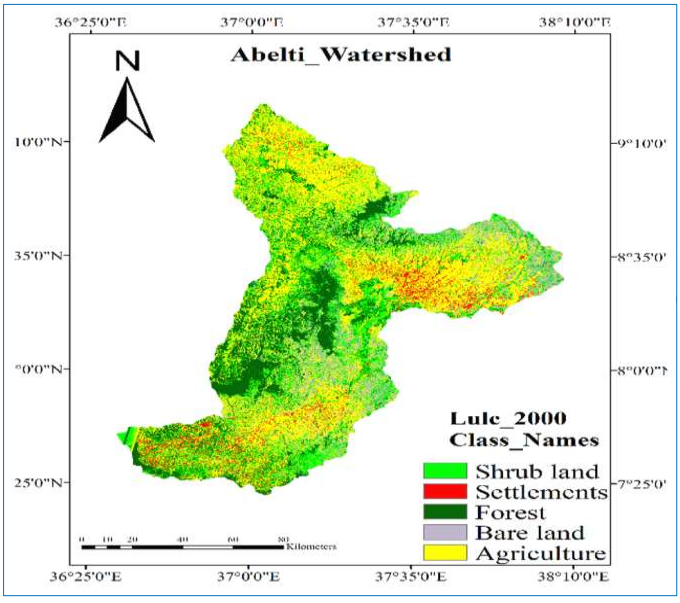

Fig. 11. LULC maps of the watershed for 2000

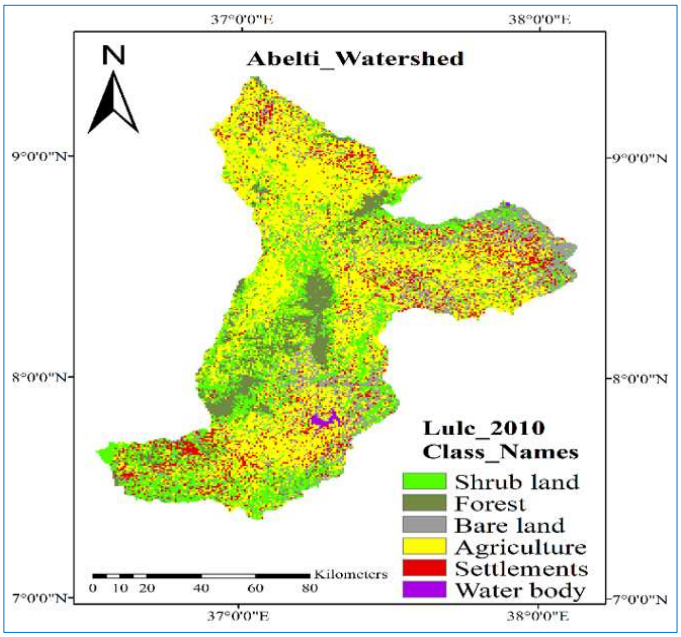

Fig. 12. LULC maps of the watershed for 2010

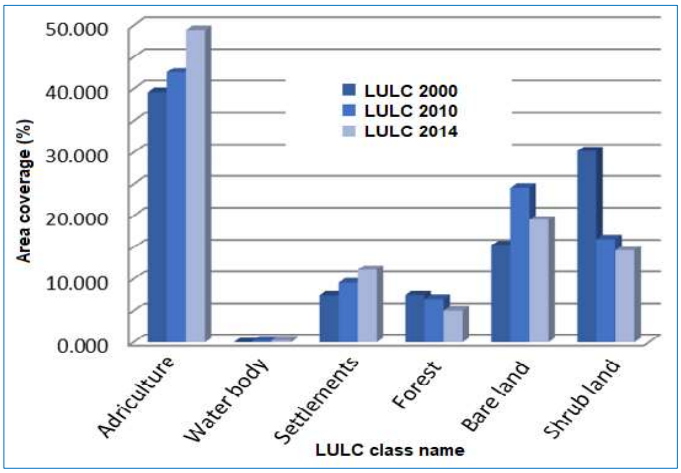

Fig. 13. LULC distribution of 2000, 2010 and 2017

Table 5. Summary of LULC change analysis of each class

LULC categories	Area of LULC classes (%)			Change detection (%)	
	2000	2010	2017	LULC (2000-2010)	LULC (2010-2017)
Agriculture	41.231	42.617	49.327	3.36	15.74
Water	0	0.283	0.297	-	4.95
Settlements	5.471	9.439	11.528	72.53	22.13
Forest	18.938	7.8	10.892	-58.81	39.64
Shrub lands	26.082	24.459	19.305	-6.22	-21.07
Bare lands	8.279	15.402	8.652	86.04	-43.83

2.10. SWAT Calibration and Uncertainty Programs (SWAT-CUP)

The SWAT-CUP is an interface of SWAT by which any calibration, uncertainty and sensitivity program can easily be linked with SWAT model. This is demonstrated by the program links SUFI-2, GLUE, Parasol, and MCMC procedures to SWAT. In this particular study, SUFI-2 were preferred.

2.10.1. Evaluation of surface runoff

The LULC change simulation on surface runoff was the most important part of this study. To estimate the variability of surface runoff because of the LULC changes from 2000 to 2017, three different simulation runs were conducted on monthly basis by using generated LULC maps keeping other input parameters unchanged. Seasonal surface runoff because of the LULC change was evaluated and comparison was made on the surface runoff based on three simulation outputs.

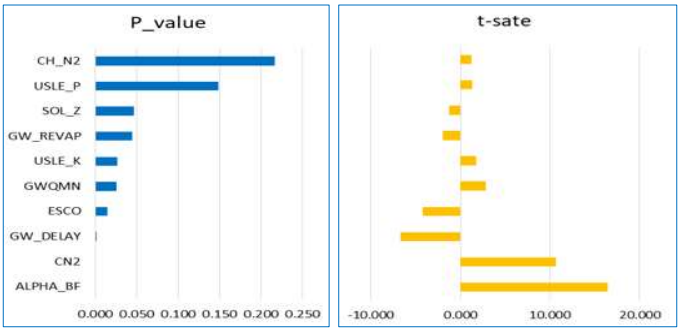

Fig. 14. Ranks of finally fitted parameters used for flow calibration and validation

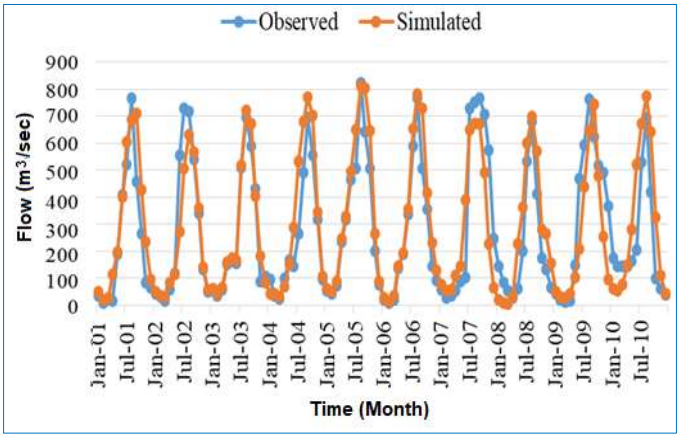

Fig. 15. Observed and simulated flow hydro graphs of calibration period (2001-2010)

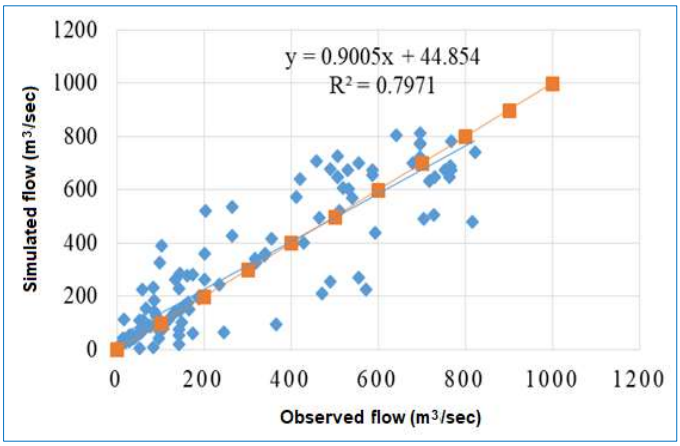

Fig. 16. Observed and simulated flow scatter plot of calibration period (2001-2010)

Table 6. Calibrated and validated model performance indicators and uncertainty measures

Simulation (months)	Uncertainty measures		Model performance indicators		
	p-factor	R-factor	R^2	NSE	PBIAS
Calibration (2001-2010)	0.76	0.71	0.79	0.78	-6.3
Validation (2011-2015)	0.85	0.62	0.92	0.85	-4.1

3. Result and Discussion

3.1. LULC classification analysis

Results of Statistics for each LULC change analysis also carried out for each year and the watershed has undergone many lands use and cover changes for recent decades as shown in the following figures (Figs. 11, 12 and 13). Forest cover decreased from 2000's to 2017 by 8.046% and the built-up area also was significantly changed between 2000 and 2017 by 6.057% due to rapid development of settlements (urban centers). The results shown that the study area was dominantly covered by agriculture with 41.23% coverage in the year 2000 as shown in Figs. 11, 12 and 13. According to the satellite imagery data, there was no significant water body which covers the land in the watershed at 2000 until the Gilgel Gibe I reservoir was constructed (Wakijra et al., 2016).

3.2. Classification accuracy assessment of LULC

Accuracy assessment was a significant step to determine the degree of 'correctness' of the classified satellite images and performed by using error or confusion matrix. The error matrix calculates the parameters like the user's accuracy, producer's accuracy, overall accuracy and the kappa coefficient. The estimated values of overall accuracy for the Landsat images of 2000, 2010 and 2017 were 86.04%, 90.75% and 89.71% respectively. In addition to overall accuracy, over all kappa coefficients for 2000, 2010 and 2017 images were 0.82, 0.88 and 0.86 respectively. Based on Anderson et al. (1976), 85% was minimum accuracy value for reliable land cover classification was. According to Susana et al. (2010), Kappa values greater than 0.80 (80%) represents strong agreement and hence, the images classification accuracy of the study was almost in strong agreement.

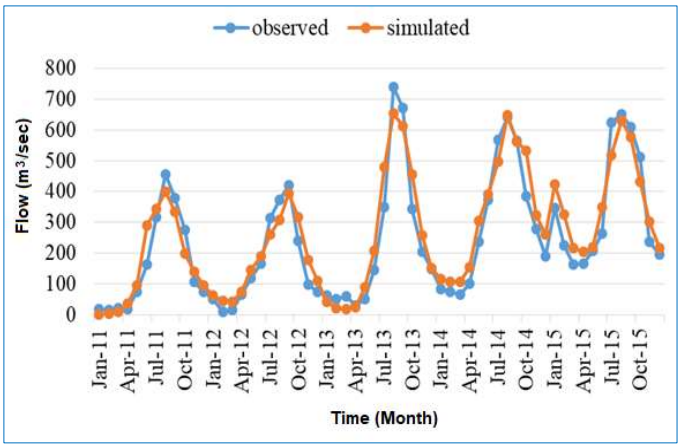

Fig. 17. Hydrograph of observed and simulated flow of validation time (2011-2015)

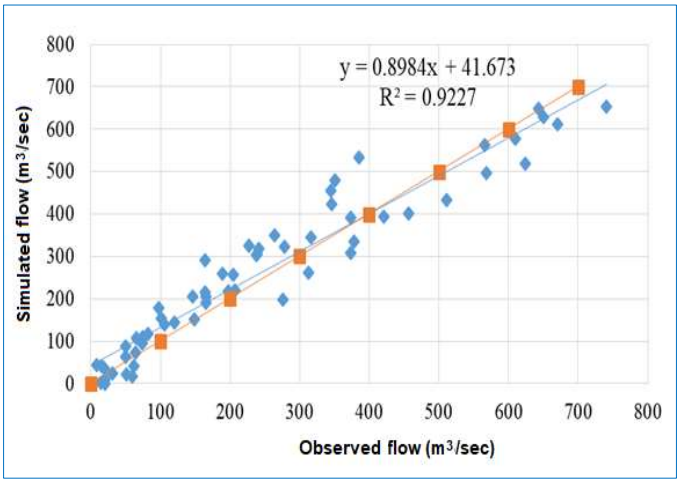

Fig. 18: Observed and simulated flow scatter plot of validation period (2011-2015)

3.3. LULC change analysis

The forest declined from 2000 to 2010 by 58.81% but increased from 2010 to 2017 by 39.64 %. The shrub land declined from 2000 to 2010 by 6.22%, from 2010 to 2017 by 21.07% and also there was a change of bare lands during the study period from 2000 to 2010 increased by 86.04% and from 2010 to 2017 decreased by 43.83% as indicated in the Table 5.

3.4. SWAT model sensitivity analysis

Hydrological model sensitivity analysis was done to know which model parameters was most sensitive in the watershed and performed for a period of ten years of the calibration (from January 1, 2001 to December 31, 2010) with two years of warm-up (from January 1, 1999 to December 31, 2000) and five years of validation (from January 1, 2011 to December 31, 2015). Based on the results obtained from sensitivity analysis using SUFI-2, the ranks of parameters assigned based on *t*-stat and *p*-value. The *p*-value indicates importance of sensitivity and *t*-stat provides the measure of parameter sensitivity (Abbaspour, 2014) as shown in Fig. 14.

After sensitive parameters were identified, auto-calibration was done for sensitive flow parameters of SWAT-CUP with generated land use and land cover map of 2010 and observed average monthly stream flow data. Correlated hydrograph and scatter plot of both simulated and observed flow were shown in Figs. 15 and 16 after auto calibration.

Table 7. Hydrological parameters from annual simulations for 2000, 2010 and 2017

Simulated hydrological parameters	LULC_2000	LULC_ 2010	LULC_2017	Change detection (%)	
				2000-2010	2010-2017
Qs (mm)	9.209	11.047	10.616	19.963	-3.898
Sw (mm)	38.435	38.304	38.615	-0.340	0.812
Qg (mm)	57.525	56.076	56.489	-2.519	0.736

Qo (m^3/sec) is stream flow, Sw (mm) is Soil moisture content, Qs (mm) is surface runoff and Qg (mm) is groundwater contribution to river flow (mm)

Table 8. Simulated dry and wet period surface runoff results of 2000, 2010 and 2017

LULC_Years		LULC_2000	LULC_2010	LULC_2017	Change detections (%)		
					2000-2010	2000-2017	2010-2017
Qs (mm)	Dry season	0.926	1.140	1.130	23.112	21.993	-0.909
	Wet season	21.707	25.881	24.908	19.233	14.749	-3.760

Table 9. Monthly simulated surface runoff using generated LULC maps of 2000, 2010 and 2017

Hydrological parameters	Year/month	Jan	Feb	Mar	Apr	May	Jun	Jul	Aug	Sep	Oct	Nov	Dec
Qs (mm)	LULC_2000	0.22	0.67	2.23	3.58	9.24	18.02	29	24.32	15	4.92	1.1	1.75
	LULC_2010	0.35	0.9	2.91	4.6	11	21.57	35	29.15	18	5.93	1.3	1.99
	LULC_2017	0.3	0.8	2.68	4.18	10.6	20.8	33	27.92	18	5.79	1.3	2.12

For model validation the remaining observed stream flow data of Gibe River at Abelti from 01 January, 2011 to 31 December, 2015 were used. The validation hydrograph and scatter plot of both simulated and observed flows were shown in Figs. 17 and 18. Calibration and validation results were shown in Table 6.

Model performance for both validation and calibration of watershed were found to be in very good agreement with the values of R^2, ENS percent PBIAS with the values of 0.79 and 0.78 and 6.3% and 0.92, 0.85 and 4.1% for calibration and validation, respectively.

3.4.1. Model responses to CULC change

3.4.1.1. Effects of LULC change on surface runoff process of the watershed

Manual calibration was done using the three LULC maps of 2000, 2010 and 2017 and optimized sensitive parameters but auto calibration was done with LULC map of 2010. LULC is significant characteristic for surface runoff process that affects soil water content, water yield, rate of infiltration, erosion, ground water flow. Understanding the effects of land use changes on surface runoff is important to know the impacts of LULC changes on watershed hydrological regimes for the watershed level. Manual calibration was

conducted to compare the modelling outputs such as surface runoff, soil water content and ground water flow as they were given in Table 7 and for the comparison of the LULC maps of 2000, 2010 and 2017.

The main objectives of the study area were to evaluate surface runoff of the watershed as shown in Table 7 under LULC change in the watershed and directly related to land cover types. Expansions of agriculture and Settlements in the watershed have the highest potential for surface runoff because the land developed impervious layer in the watershed and reduced infiltration rate of the land. Therefore, surface runoff was highly affected by land cover types and increased when the interception was less because of the forest cover decreased, surface runoff decreased when the forest cover become increased.

3.4.2. Surface runoff change under LULC change

The flow processes during different seasons under different LULC conditions of monthly average surface runoff of wet and dry months were given in Table 8. As shown in Table 9, provided/shown surface runoff was maximum during wet season but minimum during dry season whereas change of surface runoff was maximum during dry season but minimum during wet season. It can be also shown that surface runoff was maximum in months of January, July, August and September as indicated in Fig. 19 and Tables 8-9.

3.4.3. Locations of maximum surface runoff in the watershed

Land cover degradation was not uniform throughout the watershed as discussed above. Therefore, forest was dominant in north-eastern, western and middle parts of the watershed, agriculture was found at the northern, eastern and middle of southern parts of the watershed dominantly, shrub lands was found at the south eastern, north western and southern parts of the watershed, settlement areas were also found in the middle of eastern and south-western parts of the watershed and bare lands were found in the eastern and south-eastern of the watershed. Fig. 20 provides the distribution of maximum, medium and minimum surface runoff in each sub basins of the watershed and Eastern parts of the watershed has the maximum surface runoff which was covered by bare lands and agriculture for land use maps of 2000, 2010 and 2017.

Generally, from the study it is observed that LULC alteration in the form of increment of settlement areas; agricultural land and reduction of forest cover have resulted in many increases of surface runoff whereas increments of forest cover also decrease in surface runoff.

4. Conclusion

The impact of LULC change of the watershed was discussed by this study using SWAT model and ERDAS imagine 2015 integrated with ArcGIS10.1. Landsat satellite images from USGS earth explorer for the LULC maps of 2000, 2010 and 2017 were analyzed to detect land cover changes. Agriculture and settlements were continuously expanded whereas shrub lands decreased during the study periods. Therefore, from LULC analysis, it could be summarized the watershed experienced for different land use/cover changes for the last 18 years or during the study periods.

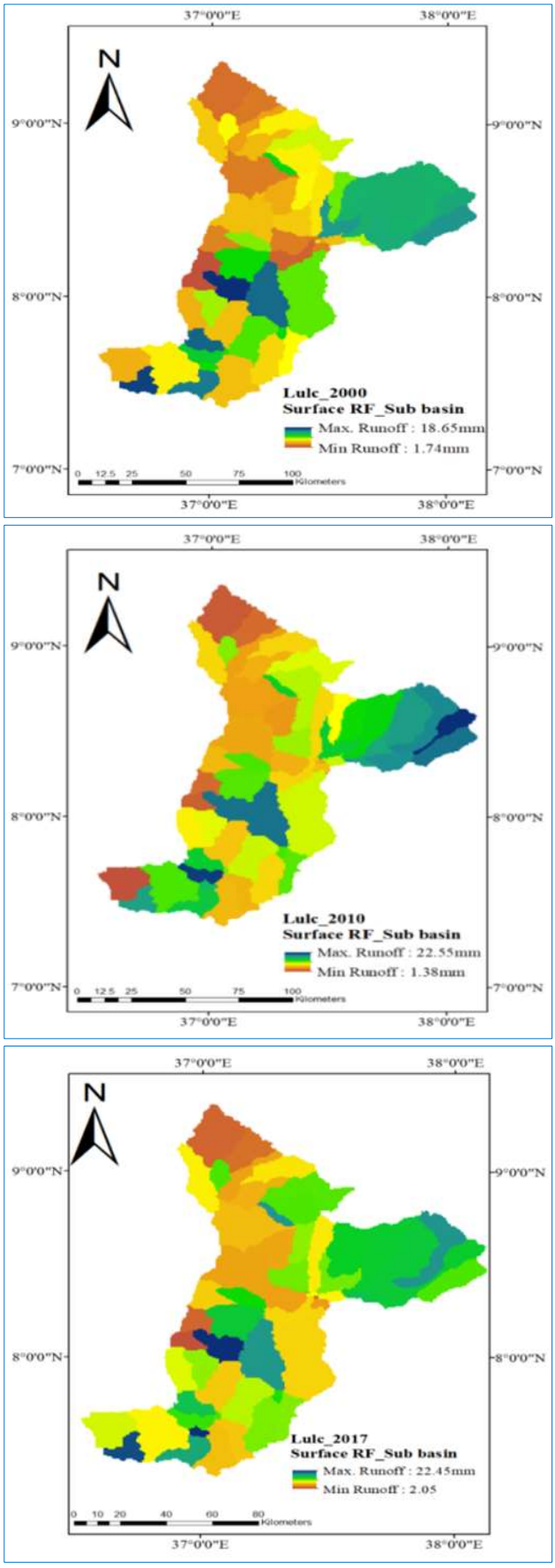

Fig. 20. Sub-basins of maximum and minimum simulated surface runoff for 2000, 2010 and 2017 LULC maps

For SWAT model simulation, meteorological data were used from 1990 to 2015 and calibration and validation were performed using flow data from January 1, 2001 to December 30, 2010 and from January 1,2011 to December 30, 2015, respectively on monthly basis. After sensitive parameters were identified, auto-calibration was done for identified sensitive parameters of SWAT-CUP with observed mean monthly stream flow data and generated land use and land cover map of 2010 then manual calibration using identified and updated sensitive parameters with generated land use and cover maps of 2000, 2010 and 2017.

In general, as obtained from the result, surface runoff was very high during wet season (July, August, June and September) and very low during dry season (November, December January and February). It can also be concluded that from the results of surface runoff, spatial and temporal distribution or change of land use/cover class plays the crucial role for the change of surface runoff in the watershed.

5. Recommendation

The dynamic change of LULC change occurred due to unproportioned population growth and various demands of the household. To solve this problem and have balanced ecological systems in the study area, family program or planning have been given widely and continuously with formal and informal education at school and other social gathering institutions or areas and awareness should also be given about natural resources protection and its importance to ecological imbalance. This research focuses on hydrological response units' estimation with only considering LULC changes keeping other factors constant, but it is highly recommended that the combined effects of sediment and climate also important in addition to LULC change to get better results for the better mitigation measurements by different stakeholders.

References

Abbaspour, K., 2014. User Manual for SWAT-CUP, SWAT Calibration and Uncertainty Analysis Programs. Swiss Federal Institute of Aquatic Science and Technology, Duebendorf Switzerland, pp 101.

Alemu, B., 2015. The Effect of Land Use Land Cover Change on Land Degradation in the Highlands of Ethiopia. Journal of Environment and Earth Science 5 (1), 2015 (1-10).

Anderson, J.R., Hardy, E.E., Roach, J.T., Witmer, R.E., 1976. A Land Use and Land Cover Classification System for Use with Remote Sensor Data. Geological Survey Professional Paper 964, Unites States Government Printing Office, Washington DC, USA.

Chalachew, A., Gudina, L., Debela, H., 2015. Analysis of land use/cover dynamics in Jimma city, Southwest Ethiopia: an application of satellite remote sensing. Ethiopian Journal of Applied Science and Technology 6 (2), 23-33.

FAO, 1995. Digital Soil Map of the World and Derived Soil Properties, (version 3.5) CD ROM. Food and Agriculture Organization of the United Nations, Rome, Italy.

Gayathri, K.D., Ganasri, B.P., Dwarakish, G.S., 2015. A Review on Hydrological Models. International Conference on Water Resources Coastal and Ocean Engineering (ICWRCOE 2015). Aquatic Procedia 4 (2015), 1001-1007.

Githu, F.W., 2007. Assessing the impacts of environmental change on the hydrology of the Nzoia catchment, in the Lake Victoria Basin. PhD Thesis, Department of Hydrology and Hydraulic Engineering, Faculty of Engineering, Vrije Universities Brussel, Belgium.

Gupta, H., Sorooshian, S., Yapo, P., 1999. Status of automatic calibration for hydrologic models: Comparison with multilevel expert calibration. Journal of Hydrologic Engineering 4 (2), 135-143. Doi: 10.1061/(ASCE)1084-0699(1999)4:2(135).

Hadgu, K.M., 2008. Temporal and spatial changes in land use patterns and biodiversity in relation to farm productivity at multiple scales in Tigray, Ethiopia. PhD Thesis Wageningen University, Wageningen, the Netherlands.

James, L.D., Burges, S.J., 1982. Selection, Calibration, Testing of Hydrologic Models. In: Hydrologic Modeling of Small Watersheds, C.T. Haan, H.P. Johnson and D.L. Brakensiek (Editors). ASAE Monograph, St. Joseph, Michigan, 437-472 pp.

Moriasi, D.N., Arnold, J.G., Van Liew, M.W., Bingner, R.L., Harmel, R.D., Veith, T.L., 2007. Model evaluation guidelines for systematic quantification of accuracy in Watershed simulations. American Society of Agricultural and Biological Engineers 50 (3), 850-900. Doi: 10.13031/2013.23153.

Palmer, M., 2002. Land Use/Land Cover Classification of Landsat 7 imagery on a Portion of Auglaize River Watershed for Input to SWAT Model. University of Toledo, Department of Geography and Planning, Toledo, USA.

RichardWoodroof and Associates, 1996. Omo-Gibe River basin Integrated Development Master Plan Study Final Report, Volume VI, Water Resources Surveys and Inventories, Ministry of Water Resources of the Federal Democratic Republic of Ethiopia, Addis Ababa, Ethiopia.

Rientjes, T.H.M., Haile, A.T., Mannaerts, C.M.M., Kebede, E., Habib, E., 2010. Changes in land cover and stream flows in Gigel Abbay Catchment, Upper Blue Nile Basin - Ethiopia. Hydrology and Earth System Sciences Discussions 7, 9567-9598.

Samuel, K.B., Abdella, K., Santosh, M.P, 2018. Impact of Land Use/Land Cover Change on Watershed Hydrology: A Case Study of Upper Awash Basin, Ethiopia. Ethiopian Journal of Water Science and Technology 1 (1), 3-26.

Santhi, C., Arnold, J., Williams, J., Dugas, W., Srinivasan, R., Hauck, L., 2001. Validation of the SWAT model on a large river basin with point and nonpoint sources. Journal of the American Water Resources 37 (5), 1169-1188.

Susana, M.V., Uzay, K., Sousa, J.M., 2010. Cohen's Kappa Coefficient as a Performance Measure for Feature Selection. IEEE International Conference on Fuzzy Systems (FUZZ-IEEE), 18-23 July 2010, Barcelona, Spain.

Wakjira, T., Tamene, A., Dawud, T., 2016. Land use land cover change Analysis using Multi Temporal Landsat data in Gilgel Gibe, Omo Gibe Basin, Ethiopia. International Journal of Sciences and Technology 5 (7), 309-323.